

# Fatigue Behavior of Open-holed CFRP Laminates with Self-healing Functionalities

A. Kotrotsos, A. Sousanis, G. Sotiriades and V. Kostopoulos\*

Applied Mechanics Laboratory, Department of Mechanical Engineering and Aeronautics, University of Patras, 26504, Rio-Patras, Greece

\*Corresponding author, e-mail address: [kostopoulos@mech.upatras.gr](mailto:kostopoulos@mech.upatras.gr)

Web Page: [http://www.mead.upatras.gr/lang\\_en/labs/view\\_details/1](http://www.mead.upatras.gr/lang_en/labs/view_details/1)

**Keywords:** CFRPs, fatigue behaviour, open hole, damage tolerance, self-healing, bis-maleimides, supramolecular polymers

## Abstract

Bis-maleimides (BMI) and Supramolecular polymers (SP) exhibit healing functionalities on polymer level. In the current investigation, the effect of both polymers into high performance aerospace carbon fiber reinforced plastics (CFRPs) is assessed. More precisely, BMI and SP modified samples having [45/-45/0/90]<sub>2S</sub> stacking sequence, with similar fiber volume fractions have been tested under quasi static tensile and tension-tension fatigue loading conditions. According to quasi static experimental results, it was shown that the incorporation of the BMI SHA did not cause degradation to the entire composite while SP modified CFRPs exhibited decreased tensile properties. In addition, tension-tension fatigue tests revealed that the incorporation of these SHAs into composites architecture made composites to slightly extend their fatigue life. Finally, three-stage stiffness degradation was observed for all material sets while both healable composites were able to significantly extend their fatigue life after the activation of the healing cycles.

## 1. Introduction

During the last decades, fiber reinforced composites (FRPs) are year by year replacing metals due to their high specific stiffness and high strength in combination with corrosion resistance. However, a primary limitation of these composites is the poor interlaminar toughness and strength. The mismatch of anisotropic mechanical and thermal properties in between plies of different principal directions promotes out of plane stresses at the edges of the structures as well as in the cases of stringer run out, thickness variation, holes and structural stiffeners joined to composite skin, and these are only some of the candidate areas for delamination under in plane and out of plane loadings. Delaminations are among the most frequent modes of failure encountered in laminated composites [1] and are resulted either from fatigue loadings or low velocity impact events. Conventional repair techniques of composites are expensive, require extensive labor force, and cannot repair defects deep inside the material. Self-healing polymers [2] is an approach which has not yet been incorporated to commercial composites but promises to face some principal weak points.

Since the understanding of formation and propagation of damage within a composite during a fatigue test is of great importance, the fatigue behaviour of these materials has been investigated in many works according to relative literature. For example, Nixon-Pearson and Hallet [3], investigated the quasi-static and fatigue damage development of bolted-hole FRPs. In [4], Liang et al. made a comparative study related to fatigue behaviour of flax/epoxy and glass/epoxy composites. According to this investigation, it was shown that flax/epoxy composites exhibited lower fatigue endurance than

glass/epoxy ones. In addition, the overall failure of open hole tension specimens, particularly in fatigue was investigated and characterized using X-ray Computed Tomography (CT) scanning in [5]. In [6], Spearing et al. investigated the tension-tension fatigue behaviour of open holed Carbon/Epoxy and Carbon/Poly-etheretherketone (PEEK) composites using an R ratio of 0.1 while images of the damage were produced through X-radiography.

In the current investigation, the fatigue behaviour of two main categories of mendable CFRPs has been studied. More precisely, quasi-isotropic CFRPs have been tested under tension-tension fatigue loading conditions. The two categories of these mendable CFRPs that were utilized for the needs of the current study are the following; CFRPs modified with BMI grains based on Diels-Alder (DA) reaction mechanism and CFRPs modified with hydrogen-bonded SP in pre-preg form. Quasi-static open hole tensile (OHT) tests were performed in order the ultimate tensile strength (UTS) to be determined. After OHT tests, three type of open hole fatigue (OHF) tests were conducted at 0.8 UTS for each material set; tests with constant loading conditions, tests with "stops" every 10 k cycles and tests with "stops" every 10 k cycles and application of the healing cycle. All tests have been stopped at specimen's failure.

## 2. Experimental

### 2.1. Materials and methods

#### 2.1.1. Raw materials

The modified composite laminates, which are utilized for the needs of the current paper, were fabricated by UD carbon fibre/epoxy resin pre-preg CE-1007 150-38. The pre-preg tape material supplied by SGL Group, Germany having tensile strength of 2.4 GPa and axial Young modulus of 140 GPa. Two types of SHA were utilized in this investigation; the DA based BMI polymer and the hydrogen-bonded SP. More information about these SHAs can be found in [7, 8]. The melting temperatures ( $T_m$ ) of both types of SHAs was measured to be approximately 110 °C and 77°C respectively, using the Perkin-Elmer DSC 8500 differential scanning calorimeter. The DSC samples were heated from ambient temperature to 150 °C at a rate of 5 °C/min. Above  $T_m$ , the interactions between adjacent polymer chains of the material start to significantly diminish.

#### 2.1.2. Sieving process of BMI and preparation of the SP pre-preg plies

The integration process of the BMI prepolymer grains through sieving onto the CFRP plies is illustrated in Figure 4-a. The BMI polymer (Figure 4-ai) was sieved onto pre-preg' surface, as Figure 4-aii suggests. The resulting pre-preg ply containing BMI prepolymer grains on its surface is illustrated in Figure 4-aiii. On the other hand the preparation process of the SP pre-preg plies is illustrated in Figure 4-b. Raw SP pieces (Figure 4-bi) were placed on the top and bottom surfaces of dry UD carbon fabric. Then, the system was placed in between two PTFE films and converted into SP pre-preg by a two-step heating/pressing treatment (Figure 4-bii) using a hot press machine. Firstly, the system was pressed under 80 bars at 100 °C for 1h. Then, heating was stopped and the SP prepreg were left under 80 bars applied pressure overnight to cool-down and reach their final form (Figure 4-biii). SP pre-pregs were fabricated in order to facilitate the introduction of the SP SHA into the composite laminated structure.

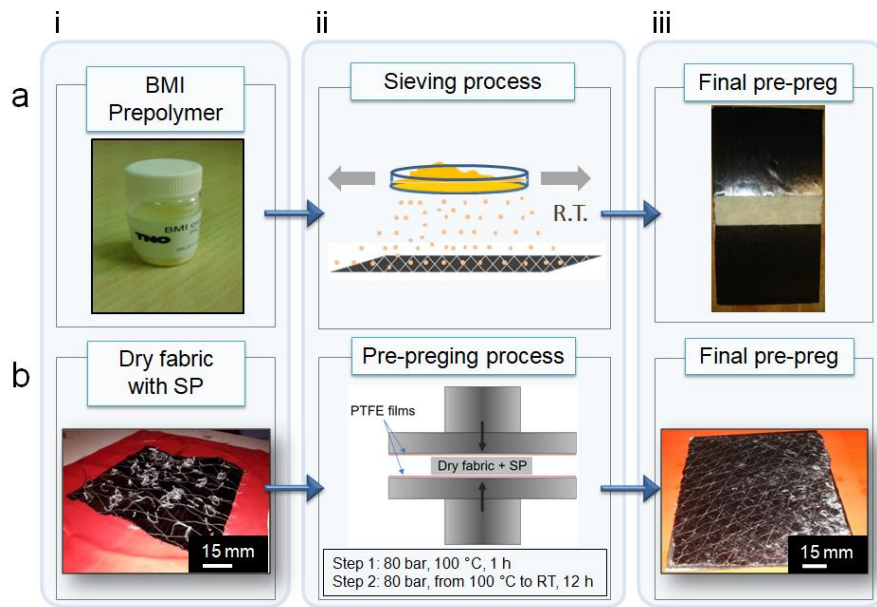


**Figure 1:** (a) Sieving process during manufacturing of modified CFRPs containing BMI prepolymer grains, (b) Preparation process of the SP modified pre-preg plies.

### 2.1.3. Open-hole tensile and tension-tension fatigue testing

A uniaxial tension test of a balanced and symmetric laminate is performed in accordance with test method D 3039/D 3039M, despite the fact that the sample contains a centrally located hole. The ultimate tensile strength is calculated based on the gross cross-sectional area, disregarding the presence of the hole. While the hole causes a stress concentration and reduced net section, it is common aerospace practice to develop notched design allow-able strengths based on gross section stress to account for various stress concentrations (fastener holes, free edges etc.) The cross-head velocity was fixed at 2 mm/min. Five samples were tested for each material type, at an Instron (250 kN) hydraulic machine. The ultimate open-hole tensile strength was determined using Eq. (1),

$$\sigma = \frac{P}{A} \text{ (MPa)} \quad (1)$$

where,  $\sigma$  is the ultimate open-hole (notched) tensile strength,  $P$  is the maximum force carried by test specimen prior to failure and  $A$  is the gross-sectional area (disregarding hole). On the other hand, tension-tension fatigue tests were performed according to D 3479/D 3479M – 96, using also an Instron (250 kN) hydraulic machine. These tests were conducted under load amplitude control, having a loading ratio of  $R=0.1$ , with identical testing conditions to quasi static tests described above. The recommended loading frequency ( $f$ ) was that of 5 Hz and ensures a self-heating of specimens ( $\Delta T$ ) of less than 10 °C during the test. Three types of fatigue tests were performed at a loading level of 0.8 of the ultimate tensile strength (UTS); tests at constant loading conditions, tests with "stops" every 10 k cycles and tests with "stops" every 10 k cycles and application of the healing cycle. All tests have been stopped at specimen's failure.

### 2.1.4. Composites quality issues

C-scan inspection was performed on all the manufactured plates. A Physical Acoustics Corporation (PAC) UT C-Scan system was used with a 5 MHz transducer. C-scan images of plates intended for both type of tests confirmed good qualities and showed absence of porosity and delaminations due to the manufacturing process.

### 2.1.5. Healing procedure

After each consecutive stop the specimens were subjected to a simple healing cycle of heating under controlled through-the-thickness compression. The cycle comprised a 5 min dwell at 150 °C for CFRPs containing BMI prepolymer while 10 min dwell at 100 °C for CFRPs containing SP in pre-preg form, both under compressive loading of 1 kN. The applied temperature was chosen to be higher than the  $T_m$  values of the SHAs, in order to be sure that both SHAs will flow within the damage and to achieve the healing effect. The aforementioned healing profiles were chosen according to SHA manufacturer's guidelines. Then, the samples were left to cool-down at room temperature (RT). After the healing cycle, the samples were tested again using the same configurations.

### 2.1.6. Test program outline

The scheduled experimental test campaign organized and realized for the needs of the current work is outlined in Figure 2. The work was divided into three study levels as already mentioned in paragraph 2.1.3. The first study level investigates the fatigue life performance of CFRPs at constant loading conditions. On the other hand, at the second study level the fatigue experiments were paused every 10 k cycles in order the damage evolution within the composite to be determined through C-scan inspections. Finally, in the third study level the same route as in the second level study was followed together with the application of the healing cycles. All samples were tested to failure. Thus, this section thoroughly investigates the effect of the healing cycles on the fatigue life performance of CFRPs.

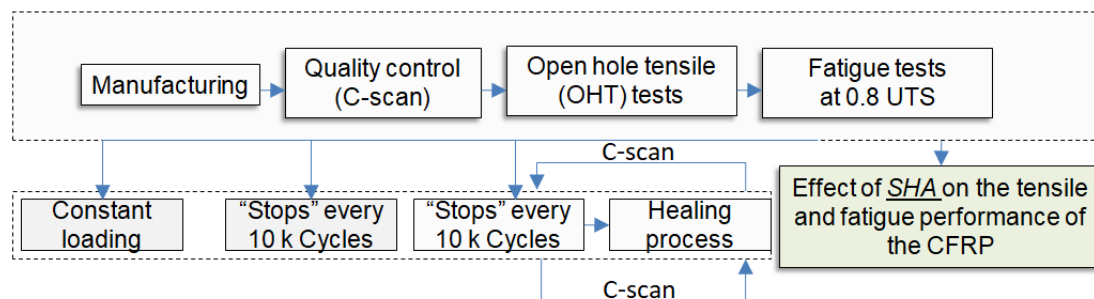
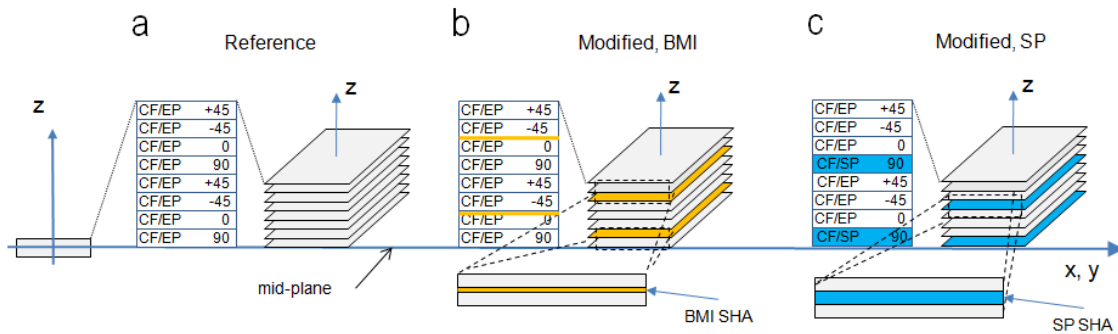


Figure 2: Schematic presentation of the scheduled characterization campaign realized in the current work.

### 2.1.7. Composites manufacturing

Three types of quasi-isotropic laminated plates containing 16 plies, with  $[45/-45/0/90]_{2S}$  stacking sequence each were manufactured for the needs of the current study; the reference laminate, the modified laminate with BMI prepolymer grains (between the primary layers of the CFRP at the amount of 120 gsm) and the modified laminate with SP prepregs. All material groups (reference and both modified) were tested under quasi-static tensile and tension-tension fatigue loading conditions. Figure 3, shows schematically the configuration of the plates (Figure 3-a) and the position where the SHAs (Figure 3-b, c, 4-c, e) were placed. The BMI prepolymer grains were placed in symmetrical fashion, in between all  $-45^0/0^0$  group layers (4 zones 38 mm wide onto the center of the pre-preg layer as presented in Figure 3-b, 4-c) within the composite structure. The SP pre-pregs replaced all  $90^0$  primary layers (as presented in Figure 3-c, 4-e)) of the composite. Following the lay-up, the laminates were vacuum bagged and cured in an autoclave for 2 h at 130 °C under 6 bars applied pressure, according to the prepreg manufacturer guidelines. The dimensions of the final plates were 300 mm × 150 mm × 2.1 mm. Five samples for each type of CFRP were exposed to quasi-static tensile tests while fifteen samples were tested under fatigue loading conditions (five samples for each category of

fatigue test described above respectively). The fiber volume fraction ( $V_f$ ) of all material sets was calculated to be close to 60%.



**Figure 3:** Design of the (a) reference CFRP, (b) the modified CFRP with BMI prepolymer and (c) the modified CFRP with SP pre-pregs.

Open hole test specimens were precisely cut out from each plate, whose geometry is illustrated in **Figure 5-b,d and f**. The hole was made by using a vertical hole drill with diameter size of 6 mm for all material sets. Special care was taken during the drilling process in order to ensure that creation of the specimen hole does not delaminate or otherwise damage the material surrounding the hole. C-scan images of samples after the drilling process showed minimal damage in areas and confirmed that samples were not affected by the mechanical loading.

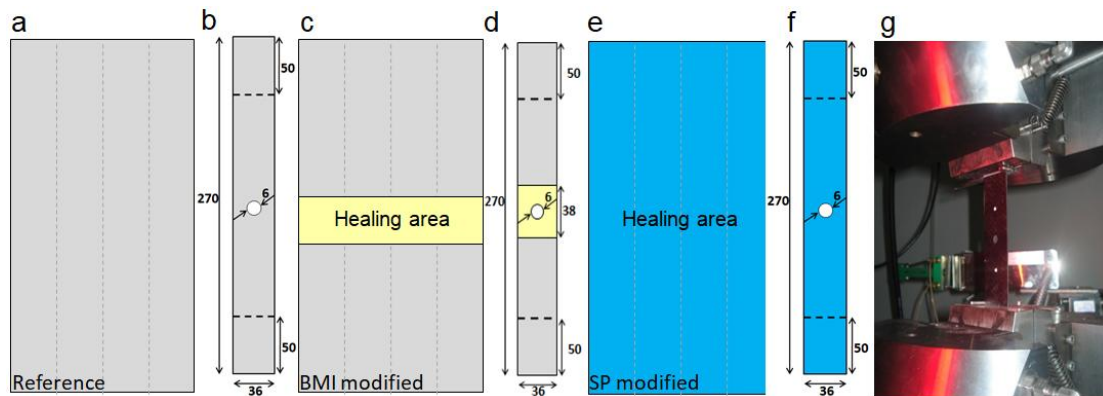


**Figure 4:** Design of (a) the reference CFRP plate, (c) the modified CFRP plate containing 4 zones of 120 gsm BMI self-healing agent (SHA) and (e) the modified CFRP plate containing 4 SP pre-pregs. Schematic depiction of (b) the reference, (d) the BMI modified and (f) the SP modified open hole specimen configuration. (g) A snapshot during the test. Dimensions in mm.

## 2.2. Results and discussion

### 2.2.1. Quasi-static tensile tests

In this paragraph, initial quasi-static tensile tests of open holed reference and both modified CFRPs are examined. For this purpose stress ( $\sigma$ ) vs. strain % ( $\epsilon$ ) measurements were performed according to specifications described in **paragraph 2.1.3**. These tests were carried out by using a batch of open

holed specimens manufactured from the same plates used in the fatigue work (that will be presented within the next paragraphs of the current section). The resulting  $\sigma$  vs.  $\varepsilon$  (%) curves are illustrated in **Figure 5-a**. For all material sets the general trend does not present any dramatic difference; the applied stress was increased linearly to failure. **Figure 5-b** compares the critical quasi-static tensile characteristics  $\sigma_{\max}$  and E for the three material sets. According to these results, it was shown that the tensile properties of CFRPs were not affected by the incorporation of the BMI prepolymer that plays the role of the SHA. More precisely, BMI modified CFRPs exhibited slightly decreased  $\sigma_{\max}$  value at the amount of 2.3% (from 661 MPa to 645 MPa) while the apparent E value was retained at the same levels for both material sets (45.4 GPa). This behaviour is attributed to the rigid and resin type nature of the SHA that made the composites not to deteriorate their mechanical properties. On the other hand, samples containing SP exhibited decreased tensile properties at the amount of almost 30% for both tensile characteristics due to the elastomeric nature of the SP material. After failure both type of samples showed a pull-out type failure mechanism which was caused by fibre failure within the  $0^{\circ}$  plies, accompanied by delamination between some of the off-axis, one or more of which failed via matrix cracking. The splitting failure of the off-axis plies propagated from the hole and occurred roughly where the fiber direction was tangential to the hole boundary.

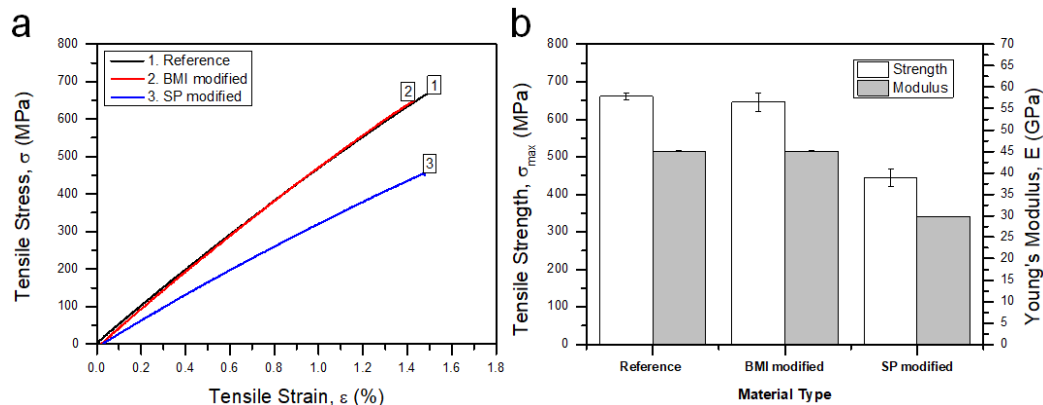


**Figure 5:** (a) Representative stress ( $\sigma$ ) vs. strain % ( $\varepsilon$ ) curves during quasi-static tensile testing of open holed reference and both modified CFRPs, (b) Comparison between the reference and both modified CFRPs in terms of the tensile strength ( $\sigma_{\max}$ ) and young's modulus (E) values, respectively.

## 2.2.2. Fatigue testing

Tension-tension fatigue tests were performed for both material sets according to specifications described in **paragraph 2.1.3**. The introduction of SHAs into the CFRP architecture is expected to have an impact on the materials' fatigue performance. At this part of work the fatigue behaviour of reference and both modified CFRPs is assessed. More precisely, fatigue tests were performed following three different routes; at constant loading conditions, with "stops" every 10 k cycles and with "stops" together with the application of the healing cycles.

### 2.2.2.1. Tension-tension fatigue behaviour of CFRPs at constant loading conditions

According to fatigue experimental results for tests conducted at constant loading conditions, it was shown that both modified samples exhibited slightly improved fatigue life by almost 8% (from 34300 to 37000 cycles respectively). This behaviour is believed to be attributed to the increase of the fracture toughness properties (both mode I and II) that the BMI and SP causes to the entire composite according to extended work presented in previous published works by the authors [9-11]. This behaviour made the composites to withstand more fatigue cycles as slightly delayed the damage evolution within the composite structure at interfaces where the maximum stiffness mismatch appears. Typical stress-strain hysteresis loops of the early ( $n/N_f=0$ ) and last loading cycles ( $n/N_f=1$ ) of reference and both modified CFRPs are presented in **Figures 6-a, b and c** respectively. In general, both material sets present similar behaviours; the loops move towards higher strains and the apparent modulus exhibit degradation due to damage evolution, for constant stress levels applied for the needs

of the current study (0.8 UTS). As it is seen in both pictures the final hysteresis loops shows significant apparent modulus degradation and the area of the loop constantly increases as expected, since it is directly related to the fatigue damage.

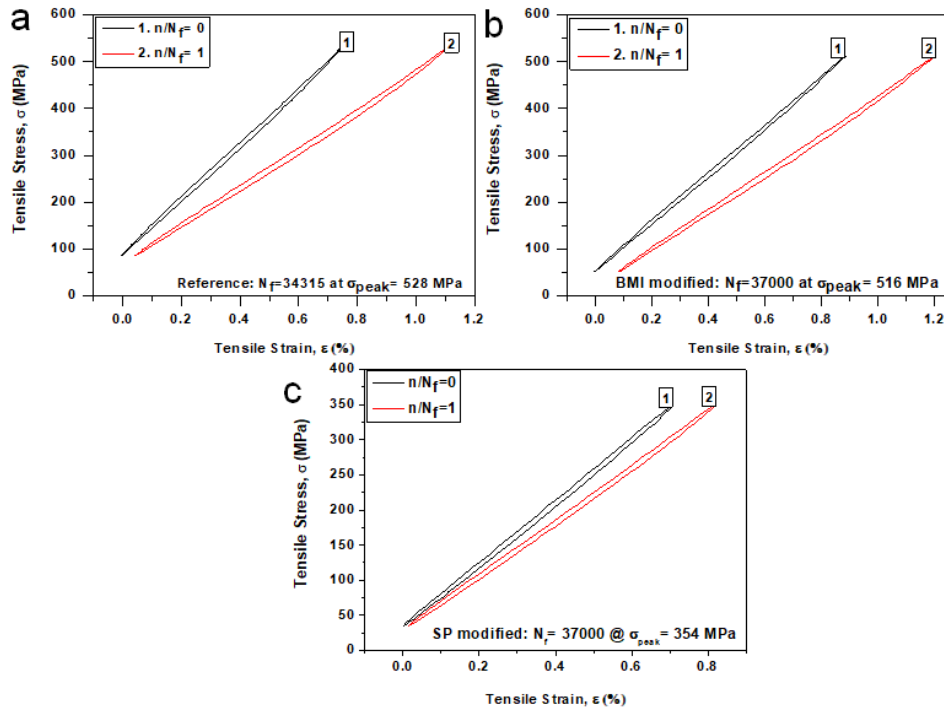


**Figure 6:** Depiction of the first and the final hysteresis loops of (a) Reference, (b) BMI modified CFRPs and (c) SP modified CFRPs at 0.8 UTS.

The plots of the maximum ( $\epsilon_{\max}$ ) and minimum ( $\epsilon_{\min}$ ) strains with respect to the life ratio are presented in **Figure 7-a**. These figures highlight a continuous increase of both strain values for all material sets (Reference and both modified ones). This behaviour is supposed to be related to the hot creep effect due to the fact that the fatigue loading consists of a positive mean stress superimposed with sinusoidal variations [12]. Because both extreme strains present almost similar trends, only the minimum strain, indicating the permanent deformation of the samples during the test is of significance. The overall development of the  $\epsilon_{\min}$  was calculated to be close to 0.04% for reference and SP modified CFRPs while and 0.084% BMI modified ones. One can observe that  $\epsilon_{\min}$  evolves into an almost quasi-linear stage for the whole life ratio up to failure. **Figure 7-b** present the normalized dynamic modulus evolution for both material sets. The evolution of the specimens' dynamic modulus is important factor as it gives valuable information on the material's damage evolution. This modulus was calculated as the slope of the straight line connecting the maximum and minimum stress tips of a hysteresis loop. **Figure 7-b** show typical and global evolutions of the normalized modulus ( $E/E_0$ ) with respect to the specimens' life ratio, where  $E$  and  $E_0$  are respectively the actual cyclic and average modulus measured during the first cycles. As expected and according to these figures, it was shown that the modulus in both cases decreases in three stages; a first and third stage with a sharp decrease of the modulus and a second steady stage (the middle one) between the other two. The modulus decrease was calculated to be close to 20% for reference and BMI modified CFRPs while for SP modified CFRPs close to 12%. This range for the decrease of the dynamic modulus is similar to the general behaviour of common CFRPs loaded under fatigue conditions according to other investigations [13].

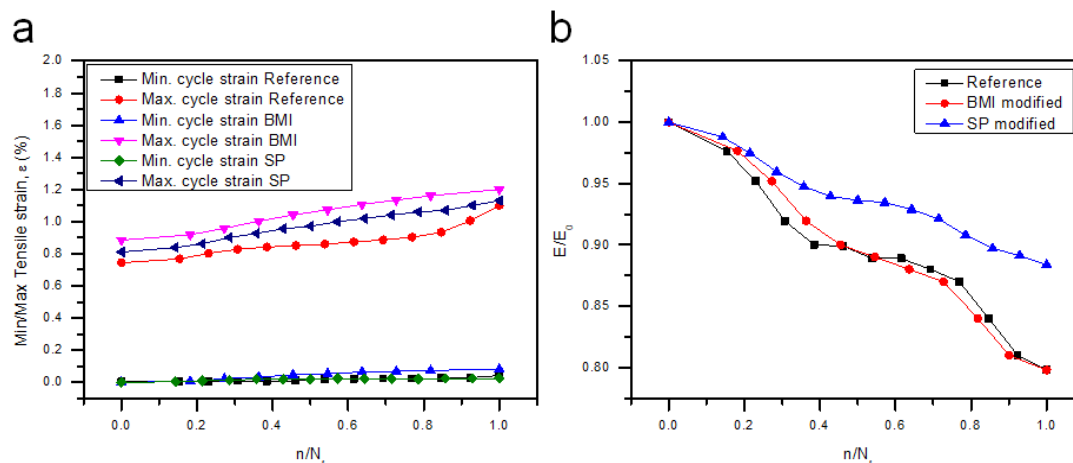
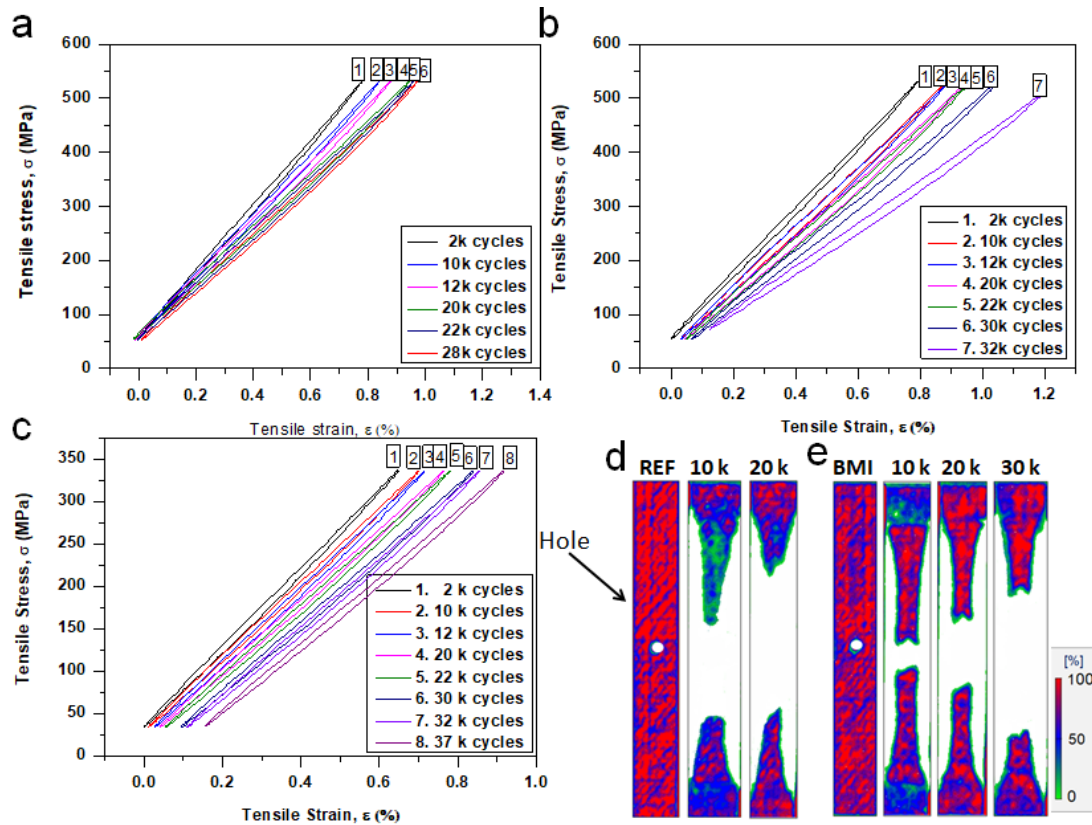


Figure 7: (a) Typical minimum and maximum cycle strains evolutions and (b) modulus ratio evolution of reference and both modified CFRPs at 0.8 UTS.

### 2.2.2.2. Tension-tension fatigue tests with "stops"

In this section, tension-tension fatigue experiments with interruptions every 10 k cycles were performed according to specifications described in paragraph 2.1.3, for both material sets. Results for reference and both modified CFRPs are presented in Figure 8. In this type of experiments, the damage evolution within the composite was determined through C-scan inspections after each consecutive stop applied to the fatigue loading of the samples. The white regions represent the damage areas induced by the fatigue loading.

Typical stress-strain hysteresis loops of the early and last loading cycles after each consecutive stop for reference, BMI modified and SP modified CFRPs are illustrated in Figure 8-a, b and c respectively. In general, the trend does not significantly differ with that observed at constant loading conditions. The hysteresis loops move towards higher strains for the constant stress levels applied to the specimens during the fatigue loading. Also as it is seen, the hysteresis loops gradually moved very far from the first cycle. The overall development of the  $\epsilon_{\min}$  for all material sets was calculated to be 0.027%, 0.084% and 0.15% for reference, BMI modified and SP modified respectively. The  $\epsilon_{\min}$  curves are not presented here but evolve into an analogous almost quasi-linear stage for the whole life ratio up to failure, as shown in Figure 7-a. The global evolution of the normalized modulus ( $E/E_0$ ) with respect to the specimens' life ratio presented an analogous behaviour with that observed at constant loading conditions (Figure 7-b). According to these results, it was shown that the modulus also decreased in three stages; a first and third stage with a sharp decrease of the modulus and a second steady stage between the other two. The loss of the modulus was calculated to be approximately 20% for reference and BMI modified CFRPs while SP modified CFRPs exhibited 25% reduction. Finally, typical C-scans for reference and BMI modified samples prior and after each consecutive stop during the fatigue experiments are depicted in Figure 8-d and e. The damage evolution within the composite structure is prominent according to these images provided. At this point, it must be mentioned that C-scan images were not able to be obtained for SP modified samples. The high SP quantity (4 pre-pregs) within the composite structure led to wave energy absorption during C-scan process.



**Figure 8:** Tension-tension fatigue experiments with “stops” every 10 k cycles for (a) Reference, (b) BMI modified and (c) SP modified CFRPs at 0.8 UTS. First and final hysteresis loops after each consecutive “stop” during fatigue experiments. C-scan inspection images after each consecutive “stop” for (d) Reference and (e) BMI modified CFRPS in order the damage area within the composite structure to be determined.

To summarize, both material sets exhibited similar behaviours at both continuous loading and loading with stop and go according to results discussed above. The main difference was that reference and BMI modified CFRPs during fatigue tests with stops exhibited slightly decreased fatigue life, if compared with them tested under constant loading conditions (13-18% reduction). Only SP modified samples exhibited the same fatigue life (37 k cycles) in both cases. This is not a usually expected behaviour, where under interrupted fatigue loading the life of the material normally extends. However, in the present case one has to take into consideration the used high  $\sigma_{max}$  which is at the level of 0.8 UTS. This behaviour (scatter in results) which is clearly visible is also attributed to the nature of fiber reinforced composites. Composite materials are known to show scatter in their fatigue lives due to statistical variations in the rate of damage development [14].

### 2.2.2.3. Tension-tension fatigue tests with "stops", healing activation and assessment of healing functionality

In the current section, tension-tension fatigue experiments with stops every 10 k cycles together with the application of the healing cycles are provided. These tests were performed only for samples having healing functionality (BMI and SP modified samples), according to specifications described in paragraph 2.1.3. Results for this type of fatigue experiments are presented in Figure 9. In this type of experiments, the damage evolution within the composite was determined through C-scan inspections after each consecutive stop. The damage recovery was also determined through C-scan inspections prior and after the each healing cycle applied to the samples.

Typical stress-strain hysteresis loops of the early and last loading cycles for BMI and SP modified CFRPs, after each consecutive stop and healing activation are illustrated in Figure 9-a and b respectively. In general, the trend does not significantly differ with that observed at other type of fatigue tests described previously (at both constant loading conditions and with stops). All hysteresis loops captured move towards higher strains for the constant stress levels applied to the specimens during the fatigue loading. Also as it is seen, the consecutive hysteresis loops moved far from the first cycle. In this case, the main difference is that the application of the healing cycle after each consecutive stop retarded the damage evolution within the composite structure as a result the fatigue life of the BMI and SP CFRPs to be extended by 75% and 23% respectively (see Figure 9-a and b). This behaviour is also confirmed by C-scan inspections for BMI modified CFRPs presented in Figure 9-c, where is clearly visible that part of initial damage area has been healed. The overall development of the  $\varepsilon_{\min}$  was calculated to be close to 0.08% for both mendable composites. Global evolution of the normalized modulus ( $E/E_0$ ) with respect to the specimens life ratio is illustrated in Figure 9-d. According to this figure, it is seen that the modulus decreases in three stages; a first and third stage with a sharp decrease of the modulus and a second steady stage between the other two. The loss of the modulus was calculated to be approximately 35% and 20% for BMI and SP CFRPs respectively. Finally, after healing process the dynamic modulus presented an increase of almost 2-3% for both material sets.

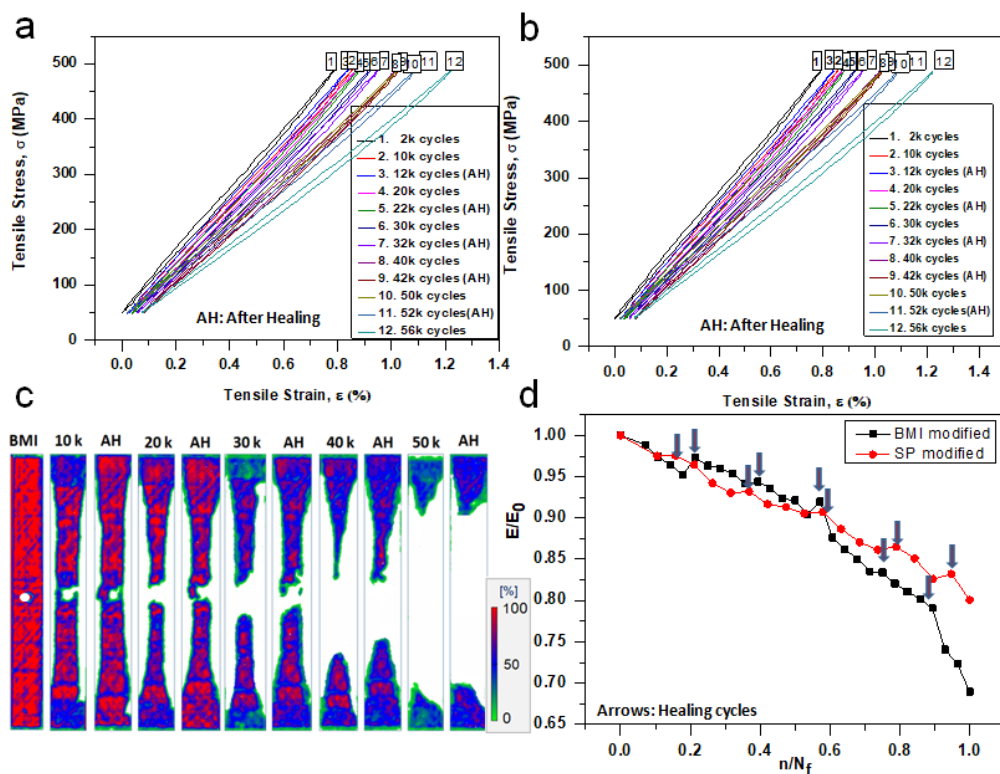


**Figure 9:** Tension-tension fatigue experiments with “stops” every 10 k cycles at 0.8 UTS for BMI and SP modified CFRPs, together with the application of the healing cycles. First and final hysteresis loops after each consecutive “stop” and healing cycle during fatigue experiments for (a) BMI modified and (b) SP modified CFRPs, (c) C-scan inspection images after each consecutive “stop” and healing cycle for BMI modified CFRPs (d) Modulus ratio evolution for both mendable CFRPs.

### 3. Conclusions

The current work, investigated the quasi-static tensile and tension-tension fatigue behaviour of notched BMI and SP modified CFRPs. According to OHT experimental results, it was shown that BMI-

modified samples exhibited tensile properties at the same levels as the reference ones while SP-modified samples slightly decreased. Tension-tension fatigue results, revealed that under constant loading conditions both modified CFRPs exhibited higher fatigue life by almost 8%. C-scan inspection images validated the increase of the induced delamination area within the composite, with the application of the fatigue cycles. In addition, all material sets exhibited a three-stage stiffness reduction with the stiffness reduction for all type of fatigue experiments. After the application of the healing process, mendable CFRPs were able to heal part of the induced delamination area according to C-scan images while extended the fatigue life of the entire composites by 75% and 23% for BMI and SP modified samples respectively, if compared with the unhealed ones tested at the same fatigue loading conditions. Finally, a slight recovery of the stiffness was observed after the application of the healing process.

## Acknowledgments

The present work has been funded by the Clean Sky 2 Programme within the frame of the project: Development of innovative and ECO-friendly airframe TECHNOLOGIES from design to manufacturing to improve aircraft life cycle environmental footprint ecoTECH, Grant Agreement number: 807083 — GAM AIR 2018 — H2020-IBA-CS2-GAMS-2017. Also, the authors thank Hartmut Fisher (TNO) and Tonny Bosman (Suprapolix) for the material supply.

## References

- [1] T.K. O'Brian. Towards a damage tolerance philosophy for composite materials and structures. *Composite Materials: Testing and Design, ASTM special technical publication*, 1059:7-33, 1990.
- [2] D.G. Bekas, K. Tsirka, D. Baltzis and A.S. Paipetis. Self-healing materials: A review of advances in materials, evaluation, characterization and monitoring techniques. *Composites Part B: Engineering*, 87:92-119, 2016.
- [3] O.J. Nixon-Pearson and S.R. Hallett. An experimental investigation into quasi-static and fatigue damage development in bolted-hole specimens. *Composites Part B*, 77: 462-473, 2015.
- [4] S. Liang, P.B. Gning and L.Guillaumat. A comparative study of fatigue behaviour of flax/epoxy and glass/epoxy composites. *Composites Science and Technology*, 72:535-543, 2012.
- [5] O.J. Nixon-Pearson, S.R. Hallett, P.J. Withers and J. Rouse. Damage development in open-hole composite specimens in fatigue. Part 1:experimental investigation. *Composite Structures*, 106:882-889, 2013.
- [6] S.M.Spearing, P.W.R. Beaumont and M.T. Kortschot. The fatigue damage mechanics of notched carbon-fiber PEEK laminates. *Composites*, 23(5):305-311, 1992 .
- [7] D.H. Turkenburg and H.R. Fischer. Diels-Alder based, thermo-reversible cross-linked epoxies for use in self-healing composites. *Polymer*, 79:187-194, 2015.
- [8] R.P. Sijbesma, F.H. Beijer, L. Brunsveld, B.J.B. Folmer, J.H.K.K. Hirschberg, R.F.M. Lange, J.K.L. Lowe and E.W. Meijer. Reversible polymers formed from self-complementary monomers using quadruple hydrogen bonding. *Science*, 278:1601-1604, 1997.
- [9] V . Kostopoulos, A. Kotrotsos, S. Tsantzalis, P. Tsokanas, T. Loutas, and A.W. Bosman. Toughening and healing of continuous fibre reinforced composites by supramolecular polymers. *Composites Science and Technology*, 2016; 128:84-93.
- [10] V. Kostopoulos, A. Kotrotsos, A. Baltopoulos, S. Tsantzalis, P. Tsokanas, T. Loutas and A.W. Bosman. Mode II fracture toughening and healing of composites using supramolecular polymer interlayers. *eXPRESS Polymer Letters*, 10(11):914-926, 2016.

- [11] V. Kostopoulos, A. Kotrotsos, S. Tsantalis, P. Tsokanas, A.C. Christopoulos and T. Loutas. Toughening and healing of continuous fibre reinforced composites with bis-maleimide based pre-pregs. *Smart Materials and Structures*, 25:84011 (12 pp), 2016.
- [12] J. Petermann and K. Schulte. The effects of creep and fatigue stress ratio on the long-term behaviour of angle-ply CFRP. *Composites Structures*, 57:205-210, 2002.
- [13] S.W. Case and K.L. Reifsnider. Fatigue of composite materials. *Comprehensive structures integrity*. Chapter 4:405-441, 2003.
- [14] N.T. Arnold and P.A. Martin Fatigue of sisal fibre reinforced composites: Constant-life diagrams and hysteresis loop capture. *Composites Science and Technology*, 68:915-924, 2008.